A high accuracy seismic modeling and RTM method on GPU

Mei Wu, Chen Lin, and Haiquan Wang, LandOcean Energy Services Co., Ltd*

Summary

The article discusses a high accuracy seismic modeling and reverse time migration (RTM) method. High-order finite-difference (FD) equation is used for modeling and RTM with fourth-order in time domain, eighth-order in x, y direction of space domain and sixteenth-order in z direction. This high-order FD solution can effectively reduce numerical dispersion. PML absorbing boundary conditions is used to effectively solve artificial boundary reflection problem. Thereby, the accuracy of modeling and RTM are significantly improved. By the advantage of GPU, the computation efficiency is largely increased. Research of theoretical data and real data shows this method is very applicable to the modeling and imaging for the media with complex surface and complex underground structure.

Introduction

Currently, Seismic numerical modeling method is based on ray theory (ray tracing method) and the numerical solutions of wave equation (Kirchhoff integral method, FD method, finite-element method and pseudo spectral method). Ray tracing method is suitable for simple medium model, but does not work well for complex geological structure. For the numerical solutions of wave equation, FD method with its high computation efficiency and versatility has become the commonly used method for seismic numerical modeling. Traditional FD method has some aspects need to be improved, such as modeling accuracy, numerical dispersion, boundary absorbing, computation capability, etc. Conventionally, second-order FD approximations are used for the time operator, but fourth-order or eighth-order FD approximations are used for the spatial operators. In this way, the result of modeling sometimes cannot reach the accuracy required.

The modeling and RTM method mentioned in this article is a high accuracy FD method. It can effectively reduce the numerical dispersions with fourth-order in time domain, eighth-order in x, y direction, sixteenth-order in z direction in space domain. PML absorbing boundary conditions is used to effectively solve artificial boundary reflection problem, improve the accuracy of modeling and RTM. By the use of GPU, the computation capability is largely increased.

Methodology

High-order finite difference equation

The motion of an acoustic wave in space and time is described by the following second-order differential equation:

$$\frac{\partial^2 u(\mathbf{x},t)}{\partial t^2} = -L^2 u(\mathbf{x},t) \qquad (1)$$

where, $-L^2 = c^2(\mathbf{x})\nabla^2$, The equation could be rewritten as following using the fourth-order Taylor-series expansions:

$$u(\mathbf{x},t+\Delta t) - 2u(\mathbf{x},t) + u(\mathbf{x},t-\Delta t) = -\Delta t^2 L^2 u(\mathbf{x},t) + \frac{\Delta t^4}{12} L^4 u(\mathbf{x},t) \qquad (2)$$

with second-order and fourth-order finite difference terms in time domain reserved (Etgen,1986). In order to further increase frequency in z-direction without sacrificing efficiency too much, we adopt the wave equation with eighth-order in both x and y direction, and sixteenth-order in z-direction.

With the same order in spatial domain, the results of the second-order and fourth-order operator in temporal domain are displayed in Figure 1 respectively. It can clearly see that dispersion is well reduced in fourth-order, and the quality is consequently improved.

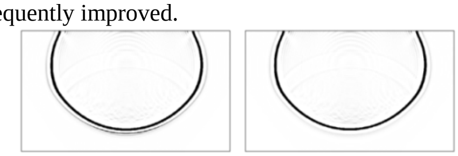

(a) (b)

Figure 1 Operators in time domain.
(a) Second-order (b) Fourth-order

PML Absorbing Boundary Conditions (ABCs)

Artificial boundary reflection is an important problem for modeling and RTM. Three approaches are employed according to different situations. For top boundary, symmetric and PML absorbing boundary conditions are adopted. Random velocity boundary is ordinarily used for lateral boundaries. But for the media with rugged surface, PML boundary must be adopted for top boundary. Equation (3) and (4) describe the propagation of energy in z-direction through the PML with loss terms:

$$\frac{\partial \Phi_x}{\partial t} + v^2\Phi_x = v^2\frac{\partial A_x}{\partial x}, \quad \frac{\partial \Phi_y}{\partial t} + v^2\Phi_y = v^2\frac{\partial A_y}{\partial y}, \quad \frac{\partial \Phi_z}{\partial t} + v^2 q\Phi_z = v^2\frac{\partial A_z}{\partial z} \qquad (3)$$

$$\frac{\partial A_x}{\partial t} = \frac{\partial(\Phi_x+\Phi_y+\Phi_z)}{\partial x}, \quad \frac{\partial A_y}{\partial t} = \frac{\partial(\Phi_x+\Phi_y+\Phi_z)}{\partial y}, \quad \frac{\partial A_z}{\partial t} + q^* A_z = \frac{\partial(\Phi_x+\Phi_y+\Phi_z)}{\partial z} \qquad (4)$$

The potential is split to $\Phi = \Phi_x + \Phi_y + \Phi_z$, A_x, A_y, A_z is temporal fields，the loss terms q and q* are attenuation coefficients (Hastings, 1996). The wavefield snapshots with PML boundary compared with symmetric boundary is shown in Figure 2. Using symmetric boundary, the artificial reflections bounce back from the up-going wave (see the location where the red arrow indicates). However, the artificial reflections are removed perfectly by using of PML boundary.

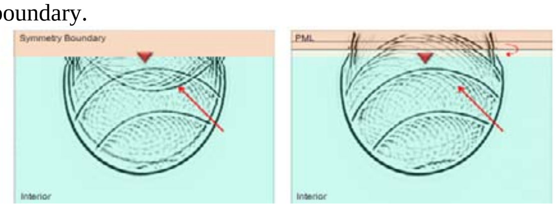

(a) (b)

Figure 2 Snapshots (a) symmetric (b) PML

GPU Implementations

Complexity and computational cost are inherent problems for modeling and RTM. With the advance of high performance computing, GPU is used to achieve massive computation capacity. GPU performance of different types is shown in figure 3. Compared with other GPU types, K10 is the best choice because of its fast computation speed, big memory, multinuclear and low cost.

Tesla GPU	K20X	K10(dual cores)	M2090
Double precision (Tflops)	1.31	0.19	0.665
Single precision (Tflops)	3.95	4.577	1.331
Memory	6GB	8GB	6GB
Cores	2688	3072	512

Figure 3 GPU performance

Shot volume is partitioned into several parts at first to fit in video memory which is 1.5GB to 6 GB. The workflow is depicted in Figure 4 (Abdelkhalek, 2009). Synchronization is essential in time marching. Two kinds of synchronization are implemented, one is data transported to share memory in each GPU, then synchronize threads, which can read neighborhood thread data from share memory; the other is data exchange between GPUs border, adding PML boundary after the synchronization.

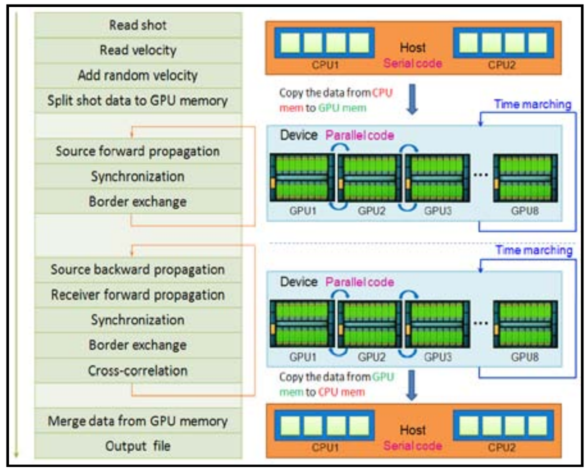

Figure 4 Workflow on GPU

Examples

In the first example, we design a 2D thin-sand body model shown in figure 6a. In this model, three geometries were designed to demonstrate the relationship between modeling accuracy and the calculation grid. Three synthetic datasets were generated by the high-order FD method mentioned in the article. The model was build with total 750 shots. The receiver interval was build with 20m, 10m, and 5m respectively, 4000m in maximum offset. The dominant frequency of Ricker wavelet used for modeling was 30Hz, 70Hz, and 120Hz, respectively. The grid spacing Δx and Δz was 10m and 4m, 5m and 2m, 2.5m and 1m, respectively. Modeling results were shown in figure 5. From the figure, we can see that the pinchout boundary of thin-sand body was obscure in modeling shot (a), clearer in shot (b) and clearly visible in shot (c). To verify the modeling results, we performed RTM for these three different modeling shots and the RTM results were shown in figure 6. In order to be seen clearly, the results were partially magnified (red box area), as shown in figure 7. The thin-sand body was hardly to be distinguished because of lower frequency in the figure 7b. Figure 7c showed that the shape of the thin-sand body was well delineated, but the boundary of thin-sand body was not clear. The pinchout boundary of thin-sand body was clearly visible and of high resolution of 1m shown in the figure 7d. Additionally, we analyzed the computation efficiency of modeling and RTM. The time used for modeling one shot for three geometries was 1.5min, 4min, and 20min respectively, and the time used for RTM one shot was 3.7min, 10min, and 36min respectively. These results indicated that the smaller the grid spacing, the higher the accuracy, and correspondingly the longer the computation time.

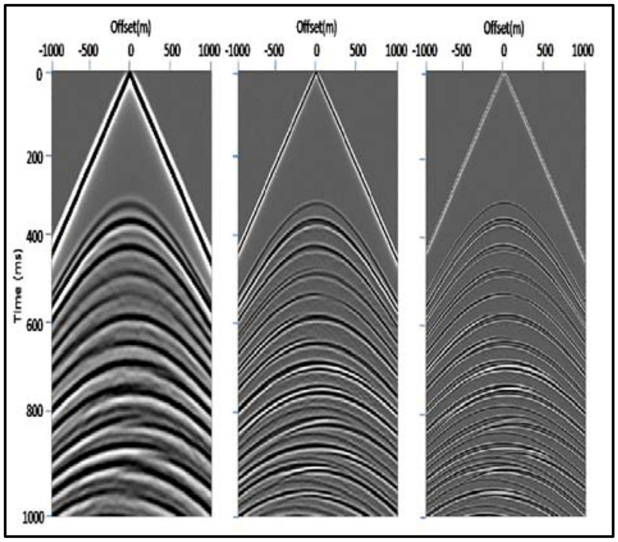

(a) (b) (c)

Figure 5 Modeling shots (a) Δx=10m, Δz=4m (b) Δx=5m, Δz=2m (c) Δx=2.5m, Δz=1m

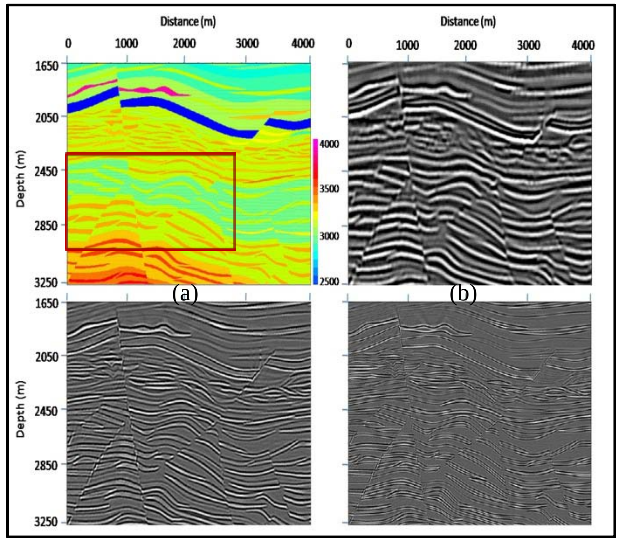

Figure 6 Velocity Model (a) and RTM result (b) Corresponding to 5a (c) Corresponding to 5b (d) Corresponding to 5c

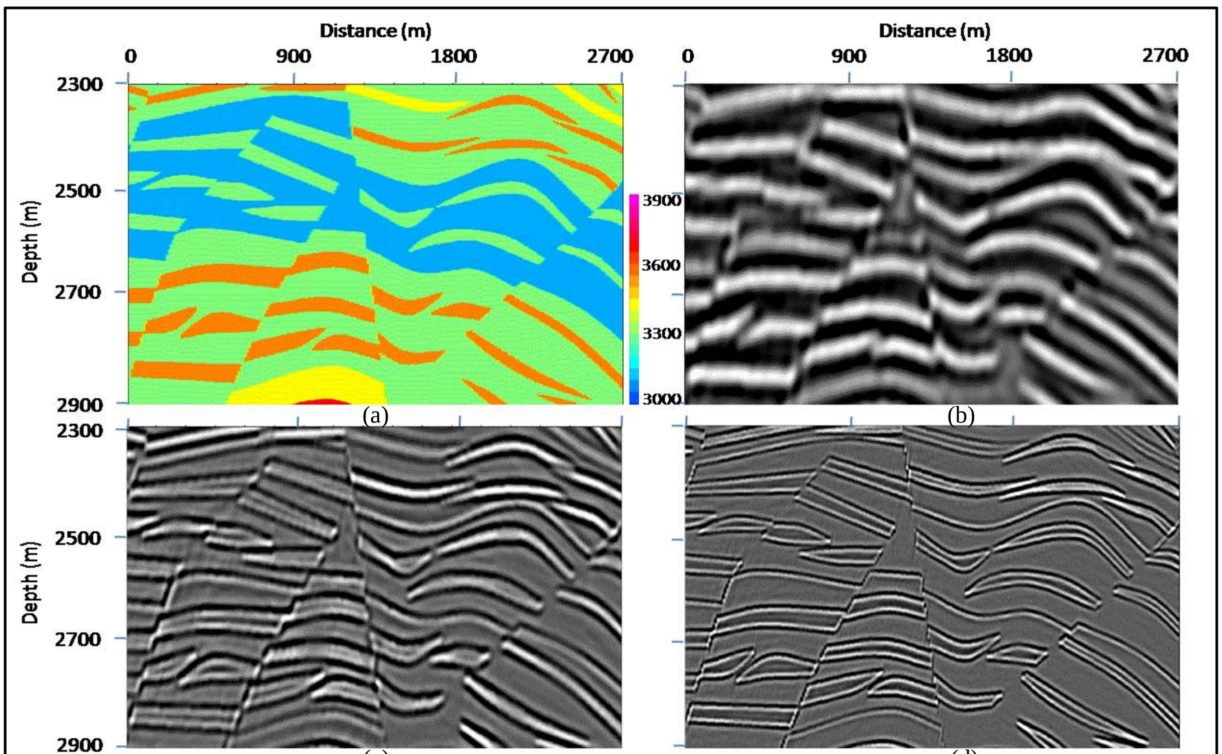

Figure 7 Velocity Model (Zoom-in display) (a) and RTM result (b) corresponding to 5b (c) corresponding to 5c (d) corresponding to 5d

The second model is a rugged surface model, as shown in figure 9 at the top. The surface was severely rugged and the maximum elevation difference reached 2000m. Velocity of the strata is changed from 3500 to 6300m/s. Total 530 shots were designed for modeling and 960 channels per shot, a receiver spacing of 15m, and 7200m maximum offset. For this kind of model, we performed modeling and RTM directly from rugged surface. The modeling results with high accuracy at three different locations were shown in figure 8. The RTM result is shown in figure 9 at the bottom. From it, we can see a good imaging of high-steep dip structure at both flanks and the overthrust at the deeper part. The boundaries of the low-velocity part in the middle were clearly delineated.

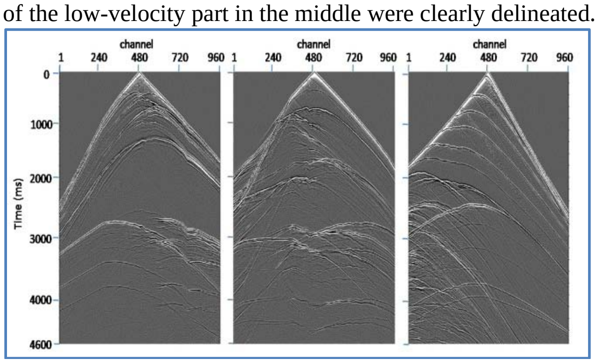

(a) Shot133 (b) Shot357 (c) Shot469

Figure 8 Modeling shots at different locations

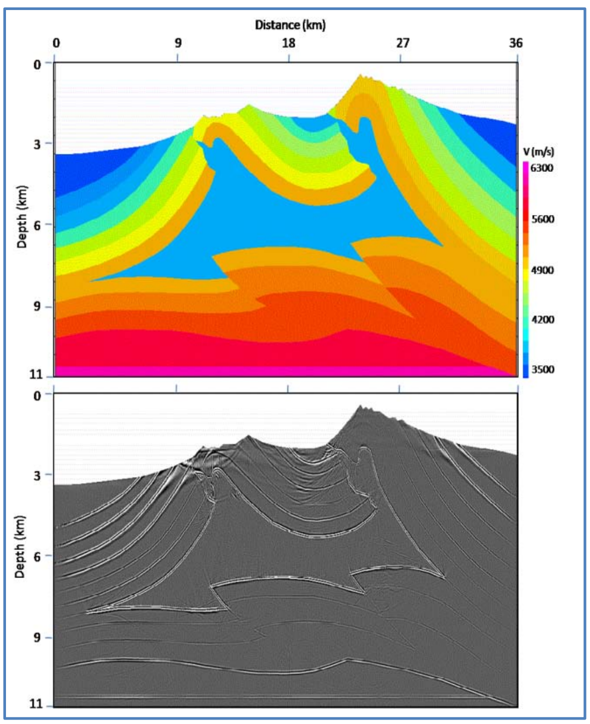

Figure 9 Rugged surface velocity model and RTM result

The third example is real 3D dataset from northwest of China. RTM (introduced in this article) processing was performed for this data. Compared with Kirchhoff PSDM result from other commercial software, RTM result was of higher quality for the imaging of steep structure (as shown in the blue circle) and overthurst (as shown in the yellow circle), see figure 10.

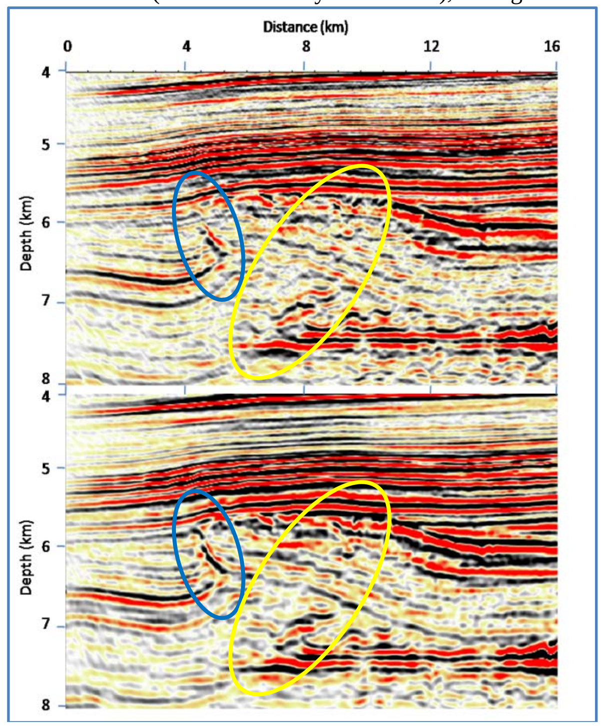

Figure 10 Kirchhoff PSDM result (top) and RTM result (bottom)

Discussions and conclusions

The method introduced in this article is a high accuracy seismic modeling and RTM method on GPU. Compared with conventional FD method, our method is of higher-order in time and space domain. By using PML absorbing boundary conditions, the accuracy of modeling and RTM is improved significantly. Furthermore, the usage of GPU largely increases computation efficiency. For 2D data, minimum grid spacing can be $1m \times 1m$ and the dominant frequency of Ricker wavelet can reach 150Hz. Using these parameters to perform modeling and RTM, the sand body of 1m thickness can be clearly distinguished. However, this high frequency is hard to obtain in field acquisition. For 3D data, because of the limitation of GPU memory, minimum grid spacing can be $10m \times 10m \times 10m$ and the highest dominant frequency of Ricker wavelet can reach 40Hz.